

Implications for relic neutralinos of the theoretical uncertainties in the neutralino–nucleon cross–section

A. Bottino^{a*}, F. Donato^b, N. Fornengo^c, S. Scopel^{d§}

^a *Dipartimento di Fisica Teorica, Università di Torino
and INFN, Sez. di Torino, Via P. Giuria 1, I-10125 Torino, Italy*

^b *Laboratoire de Physique Théorique LAPTH, B.P. 110, F-74941
Annecy-le-Vieux Cedex, France*

and INFN, Sez. di Torino, Via P. Giuria 1, I-10125 Torino, Italy

^c *Instituto de Física Corpuscular – C.S.I.C. – Departamento de Física Teòrica,
Universitat de València, E-46100 Burjassot, València, Spain*

^d *Instituto de Física Nuclear y Altas Energías, Facultad de Ciencias,
Universidad de Zaragoza, Plaza de San Francisco s/n, E-50009 Zaragoza, Spain*

Abstract

We discuss the effect induced on the neutralino–nucleon cross–section by the present uncertainties in the values of the quark masses and of the quark scalar densities in the nucleon. We examine the implications of this aspect on the determination of the neutralino cosmological properties, as derived from measurements of WIMP direct detection. We show that, within current theoretical uncertainties, the DAMA annual modulation data are compatible with a neutralino as a major dark matter component, to an extent which is even larger than the one previously derived. We also comment on implications of the mentioned uncertainties for experiments of indirect dark matter detection.

*E–mail: bottino@to.infn.it, donato@lapp.in2p3.fr, fornengo@flamenco.ific.uv.es,
scopel@posta.unizar.es

§INFN Post–doctoral Fellow

I. INTRODUCTION

The sensitivities of the experiments of direct search for WIMPs have remarkably improved in recent years, allowing now the exploration of sizeable regions of the physical parameter space of specific particle candidates for dark matter. This is the case of the neutralino [1], for which some direct detection experiments are already capable of investigating significant features in domains of the parameter space which are also under current exploration at LEP2.

The signal searched for in experiments of WIMP direct detection is a convolution of the WIMP velocity distribution in the halo with the quantity $\rho_\chi \sigma_{el}$, where ρ_χ is the local WIMP matter density [2] and σ_{el} is the WIMP–nucleus elastic cross–section. Under the assumption that the WIMP has the two following properties: i) its cross–section with matter is dominated by coherent effects, ii) its (spin-independent) couplings are essentially the same for protons as for neutrons, then one can straightforwardly factor out a scalar (spin-independent) WIMP–*nucleon* cross–section, $\sigma_{\text{scalar}}^{(\text{nucleon})}$, in σ_{el} . In this instance, the information derivable from any experiment of WIMP direct search may be directly formulated in terms of the quantity $\rho_\chi \sigma_{\text{scalar}}^{(\text{nucleon})}$, and the sensitivities of various experiments may be easily compared among each other [3]. Properties i) and ii) are actually satisfied almost everywhere in the supersymmetric parameter space [4], when the WIMP candidate is a neutralino, which is the case explicitly discussed in the present paper.

Some of the WIMP direct search experiments are already sensitive, or are on the verge of becoming sensitive, to the range $\rho_\chi^{0.3} \sigma_{\text{scalar}}^{(\text{nucleon})} \sim \text{a few} \cdot 10^{-9} \div 1 \cdot 10^{-8}$ nbarn, where $\rho_\chi^{0.3}$ denotes the local density normalized to the standard value of 0.3 GeV cm^{-3} . This goal has already been achieved by the DAMA experiment [5], which has reported the indication of an annual modulation effect in its counting rate, compatible with values of the quantity $\rho_\chi^{0.3} \sigma_{\text{scalar}}^{(\text{nucleon})}$ in the range

$$3 \cdot 10^{-9} \text{ nbarn} \lesssim \rho_\chi^{0.3} \sigma_{\text{scalar}}^{(\text{nucleon})} \lesssim 1 \cdot 10^{-8} \text{ nbarn}, \quad (1)$$

for values of the WIMP mass, correlated with $\rho_\chi^{0.3} \sigma_{\text{scalar}}^{(\text{nucleon})}$, which extend over the range $30 \text{ GeV} \lesssim m_\chi \lesssim 130 \text{ GeV}$ [6]. The region in the $m_\chi - \rho_\chi^{0.3} \sigma_{\text{scalar}}^{(\text{nucleon})}$ plane, singled out by the DAMA experiment at $2\text{-}\sigma$ C.L., is the one depicted in Fig. 2 of Ref. [6] and therein (and here) denoted by R_m . Let us also notice that, taking into account the uncertainties in the local total dark matter density: $0.1 \text{ GeV cm}^{-3} \leq \rho_l \leq 0.7 \text{ GeV cm}^{-3}$ [7], when one assumes that a single WIMP candidate saturates ρ_l , the range of Eq.(1) implies for $\sigma_{\text{scalar}}^{(\text{nucleon})}$:

$$1 \cdot 10^{-9} \text{ nbarn} \lesssim \sigma_{\text{scalar}}^{(\text{nucleon})} \lesssim 3 \cdot 10^{-8} \text{ nbarn}, \quad (2)$$

Another experiment of WIMP direct detection which is now entering the upper part of the

range of Eq.(1) for $\rho_\chi^{0.3}\sigma_{\text{scalar}}^{(\text{nucleon})}$ is the CDMS experiment [8].

Once a given range for $\rho_\chi\sigma_{\text{scalar}}^{(\text{nucleon})}$ is singled out by an experiment, what are the implications for specific particle candidates? We addressed this question in Refs. [9,6] in the case of the DAMA data, under the assumption that the reported indication of an annual modulation is interpreted in terms of an effect due to relic neutralinos. We derived a number of features for the neutralino cosmological properties, by selecting the supersymmetric configurations on the basis of the range of Eq.(1), appropriately correlated with the range of m_χ . In particular, we proved that this range for $\rho_\chi^{0.3}\sigma_{\text{scalar}}^{(\text{nucleon})}$ is compatible with a neutralino as a sizeable component of dark matter. In the derivation of this property, the role played by the correlation between $\sigma_{\text{scalar}}^{(\text{nucleon})}$ and the neutralino–neutralino annihilation cross–section, σ_{ann} , is crucial. In fact, these two cross-sections are normally both increasing or decreasing functions of the supersymmetric parameters. Since the neutralino relic abundance $\Omega_\chi h^2$ (Ω_χ is the neutralino cosmological density and h is the Hubble parameter in units of $100 \text{ km s}^{-1} \text{ Mpc}^{-1}$) is roughly inversely proportional to σ_{ann} [1], lower bounds on $\sigma_{\text{scalar}}^{(\text{nucleon})}$ entail upper bounds for the relic abundance. It is remarkable that, as mentioned above, the range of Eq.(1), singled out by the indication of annual modulation, is compatible with a neutralino relic abundance of cosmological interest [6,9].

From the previous discussion it is clear that one of the crucial ingredients in the derivation of the neutralino relic abundance from the results of direct detection experiments is $\sigma_{\text{scalar}}^{(\text{nucleon})}$. But, actually, how accurately can this quantity be evaluated at present? The point is that $\sigma_{\text{scalar}}^{(\text{nucleon})}$ usually takes dominant contributions from interaction processes, where neutralinos and quarks (inside the nucleon) interact by exchange of Higgs particles or squarks, and the relevant couplings are still plagued by sizeable uncertainties, related to hadron physics, which have not yet received satisfactory answers. Indeed, the Higgs–quark–quark or squark–quark–neutralino couplings involve the use of quark masses and quark scalar densities inside the nucleon, *i.e.* quantities which are subject to large uncertainties.

We pointed out this problem in Ref. [10], where we showed that, by taking two different determinations [11,12] of the pion–nucleon sigma term, $\sigma_{\pi N}$, and of the fractional strange content in the nucleon y (see later on for the definitions of these two quantities), these uncertainties may affect $\sigma_{\text{scalar}}^{(\text{nucleon})}$ approximately by a factor of 3. This point, subsequently also recognized in Ref. [13], was usually overlooked in subsequent papers, though the aforementioned uncertainties still persist. The common practice prevailed of employing, for the relevant couplings, some standard values, which became consolidated more because of their reiterated use, rather than because of confirmation by more refined theoretical analyses.

Actually, the quantities $\sigma_{\pi N}$ and y have recently been the object of various other calculations, based mainly on chiral perturbation theory and on QCD simulations on a lattice; however, the present situation, which is schematically revised in the next section, is still far from being clear. Thus, the Higgs–quark–quark and squark–quark–neutralino couplings are still plagued by significant uncertainties, of the order of those pointed out in Ref. [10]. In the present paper we wish to take up this problem again and, moreover, to address the

question about how sensitive are the neutralino cosmological and astrophysical properties, as derived from direct detection measurements, to the uncertainties which still affect the neutralino–nucleon cross–section.

The theoretical framework employed here is the Minimal Supersymmetric extension of the Standard Model (MSSM), with the specifications given in Refs. [9,6], to which we refer for all relevant details. Our results will mainly be given in terms of scatter plots, obtained by scanning the supersymmetric parameter space over the grid defined in Refs. [9,6]. Of particular importance for the properties discussed in the next section is the role of the neutral Higgs bosons: the two CP–even ones, h and H , and the CP–odd one, A . h and H are the main mediators of the coherent neutralino–nucleus cross–section, A is important in the neutralino–neutralino annihilation channels. The neutralino is defined as the lowest–mass linear superposition of photino ($\tilde{\gamma}$), zino (\tilde{Z}) and the two higgsino states (\tilde{H}_1° , \tilde{H}_2°)

$$\chi \equiv a_1 \tilde{\gamma} + a_2 \tilde{Z} + a_3 \tilde{H}_1^\circ + a_4 \tilde{H}_2^\circ. \quad (3)$$

To classify the nature of the neutralino, we define a parameter $P \equiv a_1^2 + a_2^2$; hereafter the neutralino is called a *gaugino*, when $P > 0.9$, is called *mixed* when $0.1 \leq P \leq 0.9$ and a *higgsino* when $P < 0.1$.

II. NEUTRALINO–NUCLEUS ELASTIC CROSS–SECTION

We recall that the neutralino–nucleon scalar cross–section is given by

$$\sigma_{\text{scalar}}^{(\text{nucleon})} = \frac{8G_F^2}{\pi} M_Z^2 m_{\text{red}}^2 \left[\frac{F_h I_h}{m_h^2} + \frac{F_H I_H}{m_H^2} + \frac{M_Z}{2} \sum_q \langle N | \bar{q} q | N \rangle \sum_i P_{\tilde{q}_i} (A_{\tilde{q}_i}^2 - B_{\tilde{q}_i}^2) \right]^2, \quad (4)$$

where the two first terms inside the brackets refer to the diagrams with h – and H –exchanges in the t–channel (the A –exchange diagram is strongly kinematically suppressed and then omitted here) [14] and the third term refers to the graphs with squark–exchanges in the s– and u–channels [15]. The mass m_{red} is the neutralino–nucleon reduced mass. Here, for simplicity, we explicitly discuss only the Higgs–mediated terms, then we do not report the expressions for the squark propagator $P_{\tilde{q}_i}$ and for the couplings $A_{\tilde{q}_i}$, $B_{\tilde{q}_i}$, which may be found in Ref. [9]. However, arguments analogous to the ones given below hold also for the squark–exchange terms, which are actually included in the numerical results reported in this paper.

The quantities $F_{h,H}$ and $I_{h,H}$ are defined as follows

$$F_h = (-a_1 \sin \theta_W + a_2 \cos \theta_W)(a_3 \sin \alpha + a_4 \cos \alpha)$$

$$\begin{aligned}
F_H &= (-a_1 \sin \theta_W + a_2 \cos \theta_W)(a_3 \cos \alpha - a_4 \sin \alpha) \\
I_{h,H} &= \sum_q k_q^{h,H} m_q \langle N | \bar{q}q | N \rangle.
\end{aligned} \tag{5}$$

The matrix elements $\langle N | \bar{q}q | N \rangle$ are meant over the nucleonic state. The angle α rotates $H_1^{(0)}$ and $H_2^{(0)}$ into h and H , and the coefficients $k_q^{h,H}$ are given by

$$\begin{aligned}
k_{u\text{-type}}^h &= \cos \alpha / \sin \beta, & k_{u\text{-type}}^H &= -\sin \alpha / \sin \beta \\
k_{d\text{-type}}^h &= -\sin \alpha / \cos \beta, & k_{d\text{-type}}^H &= -\cos \alpha / \cos \beta
\end{aligned} \tag{6}$$

for the up-type and down-type quarks, respectively.

The quantities $m_q \langle N | \bar{q}q | N \rangle$'s for the light quarks u, d, s may conveniently be expressed in terms of the pion-nucleon sigma term

$$\sigma_{\pi N} = \frac{1}{2}(m_u + m_d) \langle N | \bar{u}u + \bar{d}d | N \rangle, \tag{7}$$

the fractional strange-quark content of the nucleon

$$y = 2 \frac{\langle N | \bar{s}s | N \rangle}{\langle N | \bar{u}u + \bar{d}d | N \rangle}, \tag{8}$$

and the ratio $r = 2m_s/(m_u + m_d)$. In fact, assuming isospin invariance for quarks u and d , one has

$$m_u \langle N | \bar{u}u | N \rangle \simeq m_d \langle N | \bar{d}d | N \rangle \simeq \frac{1}{2} \sigma_{\pi N} \tag{9}$$

$$m_s \langle N | \bar{s}s | N \rangle \simeq \frac{1}{2} r y \sigma_{\pi N}. \tag{10}$$

For the heavy quarks c, b, t , using the heavy quark expansion [16], one derives

$$\begin{aligned}
m_c \langle N | \bar{c}c | N \rangle &\simeq m_b \langle N | \bar{b}b | N \rangle \simeq m_t \langle N | \bar{t}t | N \rangle \simeq \\
&\simeq \frac{2}{27} \left[m_N - \left(1 + \frac{1}{2} r y\right) \sigma_{\pi N} \right],
\end{aligned} \tag{11}$$

where m_N is the nucleon mass. The quantities $I_{h,H}$ can then be rewritten as

$$I_{h,H} = k_{u\text{-type}}^{h,H} g_u + k_{d\text{-type}}^{h,H} g_d, \tag{12}$$

where

$$g_u = \frac{4}{27} \left(m_N + \frac{19}{8} \sigma_{\pi N} - \frac{1}{2} r y \sigma_{\pi N} \right), \quad g_d = \frac{2}{27} \left(m_N + \frac{23}{4} \sigma_{\pi N} + \frac{25}{4} r y \sigma_{\pi N} \right). \tag{13}$$

We turn now to the values to be associated to $\sigma_{\pi N}$, y and r .

A. Pion–nucleon sigma term.

The quantity $\sigma_{\pi N}$ may be deduced phenomenologically from measurements of the pion–nucleon scattering; however, its derivation from the experimental data is rather involved. The customary procedure is to go through the following steps (see, for instance, Ref. [17]):

i) By use of phase–shift analysis and dispersion relations, from the experimental data of low–energy pion–nucleon scattering, one derives the quantity

$$\Sigma_{CD} \equiv \Sigma(t = 2m_\pi^2) \equiv f_\pi^2 T_{\pi N}(s = m_N^2, t = 2m_\pi^2), \quad (14)$$

where s and t are standard Mandelstam variables, m_π is the pion mass, f_π is the pion–decay constant and $T_{\pi N}$ is the (Born–subtracted) pion–nucleon scattering amplitude, calculated at the so–called Cheng–Dashen point.

ii) Modulo terms of order $\lesssim 1$ MeV, which may be safely neglected, one has

$$\Sigma_{CD} \simeq \sigma_{\pi N}(t = 2m_\pi^2), \quad (15)$$

where $\sigma_{\pi N}(t)$ is the nucleon scalar form factor, defined as

$$\sigma_{\pi N}(t = (p' - p)^2) \equiv \langle N(p') | \frac{m_u + m_d}{2} (\bar{u}u + \bar{d}d) | N(p) \rangle. \quad (16)$$

iii) The evolution of $\sigma_{\pi N}(t)$, as a function of the momentum transfer from $t = 2m_\pi^2$ to $t = 0$, provides the value of $\sigma_{\pi N} \equiv \sigma_{\pi N}(t = 0)$:

$$\sigma_{\pi N} = \sigma_{\pi N}(t = 2m_\pi^2) - \Delta\sigma. \quad (17)$$

Now, it turns out that the determinations of Σ_{CD} and $\Delta\sigma$ suffer from sizeable uncertainties.

For Σ_{CD} , apart from older calculations, we have, for instance: $\Sigma_{CD} = 56 \div 72$ MeV [18] and $\Sigma_{CD} = 59 \div 62$ MeV [12,19]. A value of Σ_{CD} on the high side ($\simeq 72$ MeV) is also favoured by a more recent evaluation [20]. Thus, one could tentatively consider the range

$$\Sigma_{CD} = 56 \div 72 \text{ MeV}. \quad (18)$$

Calculations of $\Delta\sigma$ by dispersion relation techniques provide [19] (see also [21]):

$$\Delta\sigma=15.2\pm 0.4 \text{ MeV.} \quad (19)$$

These values are much larger than the ones obtained with chiral perturbation theory at leading order $\Delta\sigma \simeq 7.5 \text{ MeV}$ [22] (see Ref. [23] for a possible explanation of this discrepancy). Furthermore, it has to be noted that $\Delta\sigma$ as deduced from lattice calculations [24] is given by $\Delta\sigma=6.6\pm 0.6 \text{ MeV}$, thus by values sizably smaller than those of Eq.(19).

Combining the range for Σ_{CD} in Eq.(18) and the value $\Delta\Sigma=15 \text{ MeV}$, we obtain for $\sigma_{\pi N}$ the range $41 \text{ MeV} \lesssim \sigma_{\pi N} \lesssim 57 \text{ MeV}$. This may be compared to the results derived in Ref. [31] using heavy quark chiral perturbation theory: $38 \text{ MeV} \lesssim \sigma_{\pi N} \lesssim 58 \text{ MeV}$ and in Ref. [26] by lattice calculations: $40 \text{ MeV} \lesssim \sigma_{\pi N} \lesssim 60 \text{ MeV}$. Thus we conclude that the value of $\sigma_{\pi N}$ is still considerably uncertain; the previous results only indicate some convergence towards the range $40 \text{ MeV} \lesssim \sigma_{\pi N} \lesssim 60 \text{ MeV}$, with an upper extreme which might be even higher ($\simeq 65 \text{ MeV}$), should one take the chiral perturbation theory result ($\Delta\sigma \simeq 7 \text{ MeV}$), instead of the dispersion–relation result (Eq.(19)). Finally, we wish to notice that recent results from higher order chiral perturbation calculations provide a large value for $\sigma_{\pi N}$: $\sigma_{\pi N} = 70 \text{ MeV}$ [27]; furthermore, use of a new pion-nucleon phase-shift analysis [28], instead of the standard one [29] would make $\sigma_{\pi N}$ to rocket to a value larger than 200 MeV [30].

B. Strange–quark content of the nucleon.

A standard way to evaluate the quantity y defined in Eq.(8) is to express it in terms of $\sigma_{\pi N}$ and of the quantity σ_0 defined as

$$\sigma_0 \equiv \frac{1}{2}(m_u + m_d) \langle N | \bar{u}u + \bar{d}d - 2\bar{s}s | N \rangle, \quad (20)$$

i.e.

$$y = 1 - \frac{\sigma_0}{\sigma_{\pi N}}. \quad (21)$$

Actually, σ_0 is a quantity related to the size of the SU(3) symmetry breaking and, as such, may be calculated either from the octet baryon masses: $\sigma_0 \simeq 33 \text{ MeV}$ [11] or with chiral perturbation theory: $\sigma_0=35\pm 5 \text{ MeV}$ [22], $\sigma_0=36\pm 7 \text{ MeV}$ [31]. For definiteness, we take

$$\sigma_0 = 30 \div 40 \text{ MeV.} \quad (22)$$

Thus, we have, for instance: $0 \leq y \leq 0.25$ for $\sigma_{\pi N}=40 \text{ MeV}$, $0.11 \leq y \leq 0.33$ for $\sigma_{\pi N}=45 \text{ MeV}$, $0.33 \leq y \leq 0.50$ for $\sigma_{\pi N}=60 \text{ MeV}$, and $0.38 \leq y \leq 0.54$ for $\sigma_{\pi N}=65 \text{ MeV}$.

We wish to remark that, by general physical arguments, one would expect for y a somewhat small value, i.e. $y \simeq 0.2\text{--}0.3$; however, apart from the results of the previous derivations, which allow values of y up to $y \simeq 0.5$, also lattice results seem to favour large values: $y=0.36\pm 0.03$ [24], $y=0.66\pm 0.15$ [26] (even reducing this latter value by $\sim 35\%$ as suggested in [24], one would still have $y \simeq 0.4\text{--}0.5$).

C. Mass ratio $r = 2m_s/(m_u + m_d)$.

As we have seen at the beginning of this section, besides $\sigma_{\pi N}$ and y a third ingredient is necessary for the evaluation of $m_q \langle N | \bar{q}q | N \rangle$ in the case of the strange quark and the heavy ones: the mass ratio $r = 2m_s/(m_u + m_d)$.

The standard derivation of this ratio is based on chiral perturbation theory. Lowest order formulae (corrected for electromagnetic effects) which give the mass ratios m_u/m_d and m_s/m_d in terms of the physical masses of the K mesons, entail, for $m_s/(m_u + m_d)$, the canonical value [32]

$$r \simeq 26. \tag{23}$$

The inclusion of next-to-leading order contributions in the chiral expansion lead to the determination [33]

$$r = 24.4 \pm 1.5. \tag{24}$$

Use of mass ratios in the evaluation of r makes these results independent of the renormalization scale. However, the validity of the chiral perturbation method relies on the hypothesis that the quark condensate is the leading order parameter of the spontaneously broken symmetry.

Other methods, most notably QCD sum rules and lattice simulations of QCD, are capable of providing evaluations of individual quark masses (not only of their ratios), though these derivations still suffer from large uncertainties. For the u and d quark masses we can quote the following results derived from QCD sum rules:

$$(m_u + m_d)(1 \text{ GeV}) = 12.0 \pm 2.5 \text{ [34]} \tag{25}$$

$$(m_u + m_d)(1 \text{ GeV}) = 15.5 \pm 2.0 \text{ [35]}. \tag{26}$$

Even more spread are the values deduced with this method by various authors for the s -quark mass [36–40]. A combination of all these derivations: $m_s(1 \text{ GeV}) = 170 \pm 50 \text{ MeV}$ [40] evidentiates how large is the uncertainty in the estimate of m_s . For sake of comparison,

we can quote some values for m_s as derived from lattice QCD: $m_s(1 \text{ GeV}) = 155 \pm 15 \text{ MeV}$ [40–42] and from the τ hadronic width: $m_s(1 \text{ GeV}) = 193 \pm 59 \text{ MeV}$ [43] and $m_s(1 \text{ GeV}) = 200 \pm 70 \text{ MeV}$ [44].

If, following Ref. [34], one uses

$$m_s(1 \text{ GeV}) = 175 \pm 25 \text{ MeV} \quad (27)$$

(which combines the results of Refs. [36,37]) and takes $m_u + m_d = 12.0 \pm 2.5$ (see Eq.(25)), one obtains

$$r = 29 \pm 7. \quad (28)$$

This result may be considered as representative of the uncertainty currently affecting the mass ratio r .

D. Size of the Higgs–quark couplings.

From Eqs.(9,10,11) and the ranges for $\sigma_{\pi N}$, y and r discussed in Sections II A–II C, we see that the quantities $m_q \langle N | \bar{q}q | N \rangle$'s are indeed affected by large uncertainties. In particular, the quantity $m_s \langle N | \bar{s}s | N \rangle$, is uncertain roughly by a factor of 3-4. This has quite significant consequences on the size of $\sigma_{\text{scalar}}^{(\text{nucleon})}$, because $m_s < N | \bar{s}s | N \rangle$ is the most important term among the $m_q < N | \bar{q}q | N \rangle$'s [47], unless $\tan \beta$ is very small (see Eqs. (6),(12),(13)).

The values of the $m_q \langle N | \bar{q}q | N \rangle$'s for a few sets of values for $\sigma_{\pi N}$, y and r are given in Table I. The first three sets are representative of values currently employed in the literature. In particular the third set (denoted here as set 1) is the one used in our previous papers [9,6] on the analysis of the DAMA annual modulation data.

Set 2 and set 3 are representative sets of values which are employed here to illustrate: i) to which extent the size of $\sigma_{\text{scalar}}^{(\text{nucleon})}$ may be increased, within the afore mentioned uncertainties, and ii) which are the ensuing implications for the neutralino cosmological properties, when these are derived from experimental data of WIMP direct detection. Thus, sets 2 and 3 are meant only to be two possible representative set of values, chosen within the current uncertainties and capable of providing large values of the quantity $m_s < N | \bar{s}s | N \rangle$. Because of the correlations, previously discussed, among $\sigma_{\text{scalar}}^{(\text{nucleon})}$, σ_{ann} and $\Omega_\chi h^2$, sets 2 and 3 are expected to provide sizeable values for the neutralino relic abundance.

A more systematic analysis of the implications for relic neutralinos of uncertainties in the Higgs–quark couplings will be feasible, only when a consistent field of variation for the correlated quantities $\sigma_{\pi N}$, y and r will emerge from a thorough and coherent QCD investigation of the problem.

III. RESULTS AND CONCLUSIONS

Let us now turn to the presentation of our results. In Fig.1.a (1.b) we give the ratio of the cross-section $\sigma_{\text{scalar}}^{(\text{nucleon})}$ calculated with set 2 (set 3), to $\sigma_{\text{scalar}}^{(\text{nucleon})}$ calculated with set 1. We see that for $(\sigma_{\text{scalar}}^{(\text{nucleon})})_{\text{set 1}}$ in the range of Eq. (2) most configurations cluster around the values $(\sigma_{\text{scalar}}^{(\text{nucleon})})_{\text{set 2}}/(\sigma_{\text{scalar}}^{(\text{nucleon})})_{\text{set 1}} \simeq 3$, $(\sigma_{\text{scalar}}^{(\text{nucleon})})_{\text{set 3}}/(\sigma_{\text{scalar}}^{(\text{nucleon})})_{\text{set 1}} \simeq 5$. Thus, we have a sizeable increase in the cross-section, when sets 2 or 3 are used instead of our set of reference (set 1), which was utilized in Refs. [9,6].

Fig.2 displays the plot of $\sigma_{\text{scalar}}^{(\text{nucleon})}$ versus $\Omega_\chi h^2$, in case of set 1 (Fig. 2a) and of set 2 (Fig. 2b). The two horizontal dashed lines delimit the range of the neutralino-nucleon cross section defined in Eq.(2). The solid vertical lines delimit the cosmologically interesting range $0.01 \leq \Omega_\chi h^2 \leq 0.7$. The two vertical dashed lines delimit the range: $0.02 \leq \Omega_\chi h^2 \leq 0.2$, which represents a particularly appealing interval, according to the most recent observations and analyses [48,49]. The overall shape of these scatter plots reflects the anticorrelation between $\sigma_{\text{scalar}}^{(\text{nucleon})}$ and $\Omega_\chi h^2$. The most relevant feature of these plots is the boundary on the top-right side. It provides the maximal values allowed for the relic density, for neutralino-nucleon cross-sections in the range of Eq. (2). Notice how the boundary extends into the region of cosmological interest more markedly in case of set 2 than in case of set 1. This is a first manifestation of the fact that the DAMA annual modulation effect is compatible with a neutralino of cosmological interest, to an extent which is even larger than the one singled out in our previous papers [9,6], where only the representative set 1 was employed. (Notice that in the present analysis, although the overall range of variation of the susy parameters is the same as in Ref. [9,6], we have optimized the numerical scanning of the parameter space in order to increase the density of configurations which fall in the region of main interest.)

These cosmological properties are further displayed in Fig. 3, which depicts the scatter plots of ρ_χ versus $\Omega_\chi h^2$. Here the two horizontal lines delimit the physical region for the total local density of non-baryonic dark matter: $0.1 \text{ GeV cm}^{-3} \leq \rho_\chi \leq 0.7 \text{ GeV cm}^{-3}$; the two slant dot-dashed lines delimit the band, where linear rescaling procedure for the local density is usually applied [9,6]. At variance with the previous scatter plots of Figs. 1-2, which refer to a generic scanning of the supersymmetric parameter space, constrained only by accelerator bounds, as discussed in Refs. [9,6], the scatter plots of Fig. 3 display the susy configurations singled out by the DAMA annual modulation data. These plots are obtained with the following procedure:

i) ρ_χ is evaluated as $\rho_\chi = [\rho_\chi \sigma_{\text{scalar}}^{(\text{nucleon})}]_{R_m} / \sigma_{\text{scalar}}^{(\text{nucleon})}$, where $[\rho_\chi \sigma_{\text{scalar}}^{(\text{nucleon})}]_{R_m}$ denotes the set of experimental values of $\rho_\chi \sigma_{\text{scalar}}^{(\text{nucleon})}$ inside the DAMA annual modulation region R_m and $\sigma_{\text{scalar}}^{(\text{nucleon})}$ is calculated with Eq.(4).

ii) To each value of ρ_χ , which then pertains to a specific supersymmetric configurations, one associates the corresponding value of $\Omega_\chi h^2$, calculated as in Ref. [50].

Therefore, with this procedure, we determine the values of ρ_χ which, for each calculated $\sigma_{\text{scalar}}^{(\text{nucleon})}$, satisfy the DAMA annual modulation data.

Fig. 3 shows that the set of supersymmetric configurations selected by the DAMA data has a significant overlap with the region of main cosmological interest: $\Omega_\chi h^2 \gtrsim 0.02$ and $0.1 \text{ GeV cm}^{-3} \leq \rho_\chi \leq 0.7 \text{ GeV cm}^{-3}$. The extent of this overlap is increasingly larger for set 2 and set 3 of Table I. By way of example, for set 3 one has that, at $\rho_\chi = 0.3 \text{ GeV cm}^{-3}$, $\Omega_\chi h^2$ may reach the value 0.3. Therefore, these results reinforce our conclusions of Ref. [9,6], *i.e.* that the DAMA annual modulation data are compatible with a neutralino as a major component of dark matter, on the average in the Universe and in our Galaxy.

The same figure shows that different situations are also possible. Specifically, for configurations which fall inside the band delimited by the slant dot–dashed lines, the neutralino would provide only a fraction of the cold dark matter both at the level of local density and at the level of the average Ω , a situation which would be possible, for instance, if the neutralino is not the unique cold dark matter particle component. On the other hand, configurations above the upper dot–dashed line and below the upper horizontal solid line would imply a stronger clustering of neutralinos in our halo as compared to their average distribution in the Universe. This situation may be considered unlikely, since in this case neutralinos could fulfill the experimental range for ρ_χ , but they would contribute only a small fraction to the cosmological cold dark matter content. Finally, configurations above the upper horizontal line are incompatible with the upper limit on the local density of dark matter in our Galaxy and must be disregarded.

Finally, we wish to add the following comments:

i) To show the effect of the current uncertainties in the Higgs–quark couplings, a few representative sets of values for the relevant quantities ($\sigma_{\pi N}$, y and r) were employed, as illustration of the implications for relic neutralinos. We have explicitly discussed situations which allow sizeable values of the neutralino relic abundance. It is clear that, within the same uncertainties, other sets of values of the relevant parameters would entail relic neutralinos of much less appealing cosmological interest. A more precise evaluation of the effects implied by the mentioned uncertainties will require a significant breakthrough in the understanding of the QCD and of other hadron aspects involved in the problem. What is lacking at present is consistency among the various determinations in $\sigma_{\pi N}$, y and r .

ii) The relevance of the implication of the mentioned uncertainties in converting information from measurements of neutralino detection to neutralino cosmological properties, discussed here for experiments of direct detection, applies also to indirect experiments at neutrino telescopes, when one looks at upgoing muons from the center of the Earth. In fact, in this case the size of the expected signal depends on the neutralino capture rates by the Earth, and then mainly on $\rho_\chi \sigma_{\text{scalar}}^{(\text{nucleon})}$.

iii) A number of experimental means, meant to search for the presence of relic neutralinos in our galaxy, look for signals (antiprotons, antideuterons, positrons, diffuse gamma–rays,

gamma lines) [1] originated by neutralino–neutralino annihilation in the halo. Thus, the relevant cross–section involved in this case is σ_{ann} . Therefore, a word of caution is in order here, for the case when the expectations for these indirect signals are based on supersymmetric configurations derived from direct detection data. In the estimate of these indirect signals, one should include the uncertainties discussed in the present paper.

ACKNOWLEDGMENTS

This work was partially supported by the Spanish DGICYT under grant number PB95–1077, by the TMR network grant ERBFMRXCT960090 of the European Union and by the Research Grants of the Italian Ministero dell’Universita’ e della Ricerca Scientifica e Tecnologica.

REFERENCES

- [1] For a review of neutralino as a dark matter particle, see, for instance, A. Bottino and N. Fornengo, *hep-ph/9904469*, Lectures given at the Fifth School on Non-Accelerator Particle Astrophysics (Abdus Salam International Centre for Theoretical Physics, Trieste, June-July 1998), to appear in the School Proceedings (Eds. R.A. Carrigan, Jr., G. Giacomelli and N. Paver).
- [2] Although a number of considerations presented in Sect. I apply to a wide class of WIMPs, the remain of the paper mainly refer to the neutralino. To simplify notations, the WIMP local density is everywhere denoted by ρ_χ , even when the identification $\text{WIMP} \equiv \chi$ is not implied. The same for the WIMP mass, which is here always denoted by m_χ .
- [3] A. Bottino, F. Donato, G. Mignola, S. Scopel, P. Belli and A. Incicchitti, *Phys. Lett.* **B402** (1997) 113.
- [4] A. Bottino, V. de Alfaro, N. Fornengo, G. Mignola and S. Scopel, *Astrop. Phys.* **2** (1994) 77.
- [5] R. Bernabei et al., *Phys. Lett.* **B424** (1998) 195; *Phys. Lett.* **B450** (1999) 448.
- [6] P. Belli, R. Bernabei, A. Bottino, F. Donato, N. Fornengo, D. Prospero and S. Scopel, *hep-ph/9903501*.
- [7] E. Gates, G. Gyuk and M.S. Turner, *Phys. Rev. Lett.* **74** (1995) 3724; *Astrophys. J. Lett.* **449** (1995) L123; *Phys. Rev.* **D53** (1996) 4138; *astro-ph/9704253*, *Proceedings of the 18th Texas Symposium on Relativistic Astrophysics*, edited by A. Olinto, J. Frieman and D. Schramm (World Scientific, to appear).
- [8] R. Schnee, talk given at the David Schramm Memorial Symposium, Inner Space/Outer Space II, FNAL, 26–29 May 1999, <http://cfpa.berkeley.edu/group/directdet/gen.html>.
- [9] A. Bottino, F. Donato, N. Fornengo and S. Scopel, *Phys. Lett.* **B423** (1998) 109; *Phys. Rev* **D59** (1999) 095004; *Phys. Rev* **D59** (1999) 095003; *Astrop. Phys.* **10** (1999) 203.
- [10] A. Bottino, V. de Alfaro, N. Fornengo, A. Morales, J. Puimedon, S. Scopel, *Mod. Phys. Lett.* **A7** (1992) 733.
- [11] T.P. Cheng, *Phys. Rev.* **D38** (1988) 2869.
- [12] J. Gasser, H. Leutwyler and M.E. Sainio, *Phys. Lett.* **B253** (1991) 252.
- [13] G. Jungman, M. Kamionkowski, K. Griest, *Phys. Rep.* **267** (1996) 195.
- [14] R. Barbieri, M. Frigeni and G.F. Giudice, *Nucl. Phys.* **B313** (1989) 725.
- [15] K. Griest, *Phys. Rev.* **D38** (1988) 2357, *Nucl. Phys.* **B313** (1989) 725.
- [16] M.A. Shifman, A.I. Vainshtein and V.I. Zacharov, *Phys. Lett.* **B78** (1978) 443; *JEPT Lett.* **22** (1975) 55.
- [17] E. Reya, *Rev. Mod. Phys.* **46** (1974) 545 .
- [18] R. Koch, *Z. Phys.* **C15** (1982) 161.
- [19] J. Gasser, H. Leutwyler and M.E. Sainio, *Phys. Lett.* **B253** (1991) 260.
- [20] M. E. Sainio, invited talk at 7th International Symposium on Meson–Nucleon Physics and the Structure of the Nucleon (MENU 97), Vancouver, Canada, 28 July– 1 August 1997, *hep/9709302*.
- [21] V. Bernard, N. Kaiser and Ulf–G. Meissner, *Z. Phys.* **C60** (1993) 111.
- [22] J. Gasser, H. Leutwyler, *Phys. Rep.* **87** (1982) 77.

- [23] J. Gasser, Talk given at Workshop on Chiral Dynamics: Theory and Experiment (ChPT 97), Mainz, Germany, 1–5 September 1997, *hep-ph/9711503*.
- [24] S.J. Dong, J.-F. Lagae and K. F. Liu, *Phys.Rev.***D54** (1996) 5496.
- [25] B. Borasoy and Ulf-G. Meissner, *Phys. Lett.***B365** (1996) 285.
- [26] M. Fukugita, Y. Kuramashi, M. Okawa and A. Ukawa, *Phys. Rev.***D51** (1995) 5319.
- [27] N. Fettes, Ulf-G. Meissner and S. Steininger, *Nucl. Phys.* **A640** (1998) 199.
- [28] SAID on-line program (Virginia Tech Partial-Wave Analysis Facility), R. Arndt et al., <http://said.phys.vt.edu>.
- [29] R. Koch, *Z. Phys.***C29** (1985) 597; R. Koch and M. Mutt, *Z. Phys.***C19** (1983) 119.
- [30] P. Büttiker and Ulf-G. Meissner, *hep-ph/9908247*.
- [31] B. Borasoy and Ulf-G. Meissner, **Ann. Phys. (NY)** **254** (1997) 192.
- [32] S. Weinberg, *Trans. New York Acad. Sci. Ser. II* **38** (1977) 185.
- [33] H. Leutwyler, *Phys. Lett.***B378** (1996) 313.
- [34] J. Bijnens, J. Prades and E. de Rafael, *Phys. Lett.* **B348** (1995) 226.
- [35] C. A. Dominguez and E. de Rafael, *Ann. Phys.* **174** (1987) 372.
- [36] K. G. Chetyrkin, C. A. Dominguez, D. Pirjol and K. Schilcher, *Phys. Rev.* **D51** (1995) 5090.
- [37] M. Jamin and M. Münz, *Z. Phys.* **C66** (1995) 633.
- [38] P. Colangelo, F. de Fazio, G. Nardulli and N. Paver, *Phys. Lett.* **B408** (1997) 340.
- [39] K. G. Chetyrkin, D. Pirjol and K. Schilcher, *Phys. Lett.* **B404** (1997) 337.
- [40] C. A. Dominguez, L. Pirovano and K. Schilcher, *Nucl. Phys. B* (Proc. Suppl) **74** (1999) 313.
- [41] V. Lubicz, *Nucl. Phys. B* (Proc. Suppl) **74** (1999) 291.
- [42] V. Giménez, *Nucl. Phys. B* (Proc. Suppl) **74** (1999) 296.
- [43] J. Prades and A. Pich, *Nucl. Phys. B* (Proc. Suppl.) **74** (1999) 309.
- [44] K. G. Chetyrkin, J. H. Kühn and A. A. Pivovarov, *hep-ph/9805335*.
- [45] L. Bergström and P. Gondolo, *Astrop.Phys.* **5** (1996) 263.
- [46] V. Berezhinsky, A. Bottino, J. Ellis, N. Fornengo, G. Mignola and S. Scopel, *Astrop.Phys.* **5** (1996) 1.
- [47] G.B. Gelmini, P. Gondolo and E. Roulet, *Nucl. Phys.* **B351** (1991) 623.
- [48] W.L. Freedman, R. Kirshner and C. Lineweaver, talks given at the International Conference of Cosmology and Particle Physics (CAPP98), CERN, June 1998, wwwth.cern.ch/capp98/programme.html; M. White, *Astrophys. J.* **506** (1998) 495; N.A. Bahcall and X. Fan, *astro-ph/9804082* to appear in National Academy of Sciences Proc.; C. Lineweaver, *astro-ph/9805326*, (to appear in *Astrophys. J. Lett.*); M. Turner, *astro-ph/9904051*.
- [49] A. Sandage *et al.*, *Astrophys. J. Lett.* **460** (1996) L15; W. L. Freedman, *astro-ph/9706072*, *Proceedings of the 18th Texas Symposium on Relativistic Astrophysics*, edited by A. Olinto, J. Frieman and D. Schramm (World Scientific, to appear). and references quoted therein.
- [50] A. Bottino, V. de Alfaro, N. Fornengo, G. Mignola and M. Pignone, *Astropart. Phys.* **2** (1994) 67.

TABLES

$\sigma_{\pi N}$ (MeV)	y	r	$m_{q_l} \langle N \bar{q}_l q_l N \rangle$ (MeV)	$m_s \langle N \bar{s} s N \rangle$ (MeV)	$m_h \langle N \bar{h} h N \rangle$ (MeV)	Ref.
45	0.28	25	23	158	55	[10]
45			27	131	56	[13,45]
45	0.33	29	23	215	50	set 1 [6,9,46]
60	0.50	29	30	435	33	set 2
65	0.50	36	33	585	21	set 3

TABLE I. Values of the matrix elements $\langle N | \bar{q} q | N \rangle$ of the quark scalar densities in the nucleon times the quark masses m_q , for a few sets of values of the pion–nucleon sigma term $\sigma_{\pi N}$, the fractional strange–quark content of the nucleon y and the quark mass ratio $r = 2m_s / (m_u + m_d)$. q_l stands for light quarks, s is the strange quark and $h = c, b, t$ denotes heavy quarks. For the light quarks, we have defined $m_{q_l} \langle N | \bar{q}_l q_l | N \rangle \equiv \frac{1}{2} [m_u \langle N | \bar{u} u | N \rangle + m_d \langle N | \bar{d} d | N \rangle]$.

FIGURE CAPTIONS

FIG. 1a. Ratio of the neutralino–nucleon scalar cross–section $\left(\sigma_{\text{scalar}}^{(\text{nucleon})}\right)_{\text{set 2}}$, calculated with the parameters of set 2 defined in Table I, to $\left(\sigma_{\text{scalar}}^{(\text{nucleon})}\right)_{\text{set 1}}$ calculated with set 1, as a function of $\left(\sigma_{\text{scalar}}^{(\text{nucleon})}\right)_{\text{set 1}}$.

FIG. 1b. The same as in Fig.1a, with set 3 instead of set 2.

FIG. 2a. Neutralino–nucleon scalar cross–section $\sigma_{\text{scalar}}^{(\text{nucleon})}$, calculated using the parameters of set 1, as a function of the neutralino relic abundance $\Omega_\chi h^2$. The two horizontal dashed lines delimit the range of the neutralino–nucleon cross section defined in Eq.(2). The two solid vertical lines delimit the interval of cosmological interest. The two vertical dashed lines delimit the preferred band for cold dark matter. The shaded region is cosmologically excluded on the basis of present limits on the age of the Universe.

FIG. 2b. The same as in Fig.2a, for the parameters of set 2.

FIG. 3a. Neutralino local density ρ_χ derived by requiring that $\rho_\chi \sigma_{\text{scalar}}^{(\text{nucleon})}$ falls inside the experimental DAMA region R_m , plotted against the neutralino relic abundance $\Omega_\chi h^2$. The quantity $\sigma_{\text{scalar}}^{(\text{nucleon})}$ is calculated with the parameters of set 1. The two horizontal lines delimit the physical range for the local density of non-baryonic dark matter. The two solid vertical lines delimit the interval of $\Omega_\chi h^2$ of cosmological interest. The two vertical dashed lines delimit the preferred band for cold dark matter. The two slant dot–dashed lines delimit the band where linear rescaling procedure is usually applied. The shaded region is cosmologically excluded on the basis of present limits on the age of the Universe. Different symbols identify different neutralino compositions: circles stand for a higgsino, crosses for a gaugino and dots for a mixed neutralino.

FIG. 3b. The same as in Fig.3a, for the parameters of set 2.

FIG. 3c. The same as in Fig.3a, for the parameters of set 3.

FIGURES

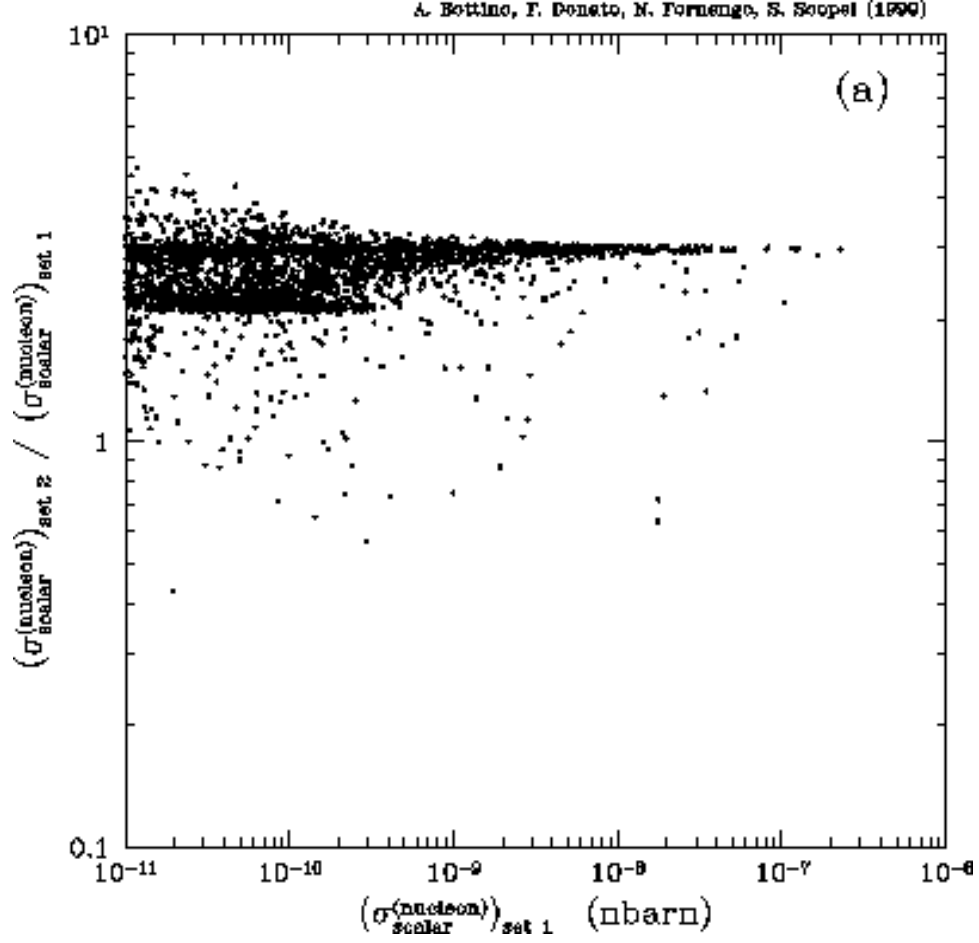


FIG.1a - Ratio of the neutralino–nucleon scalar cross–section $(\sigma_{\text{scalar}}^{(\text{nucleon})})_{\text{set 2}}$, calculated with the parameters of set 2 defined in Table I, to $(\sigma_{\text{scalar}}^{(\text{nucleon})})_{\text{set 1}}$ calculated with set 1, as a function of $(\sigma_{\text{scalar}}^{(\text{nucleon})})_{\text{set 1}}$.

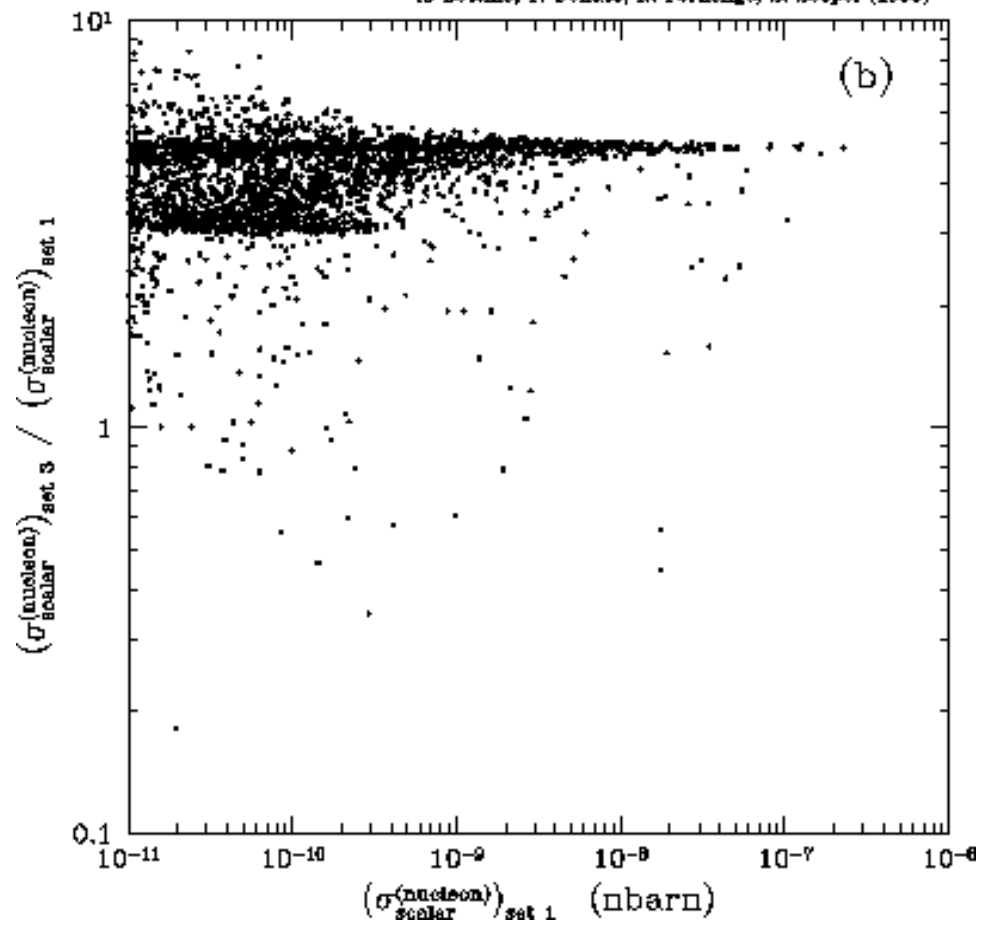


FIG.1b - The same as in Fig.1a, with set 3 instead of set 2.

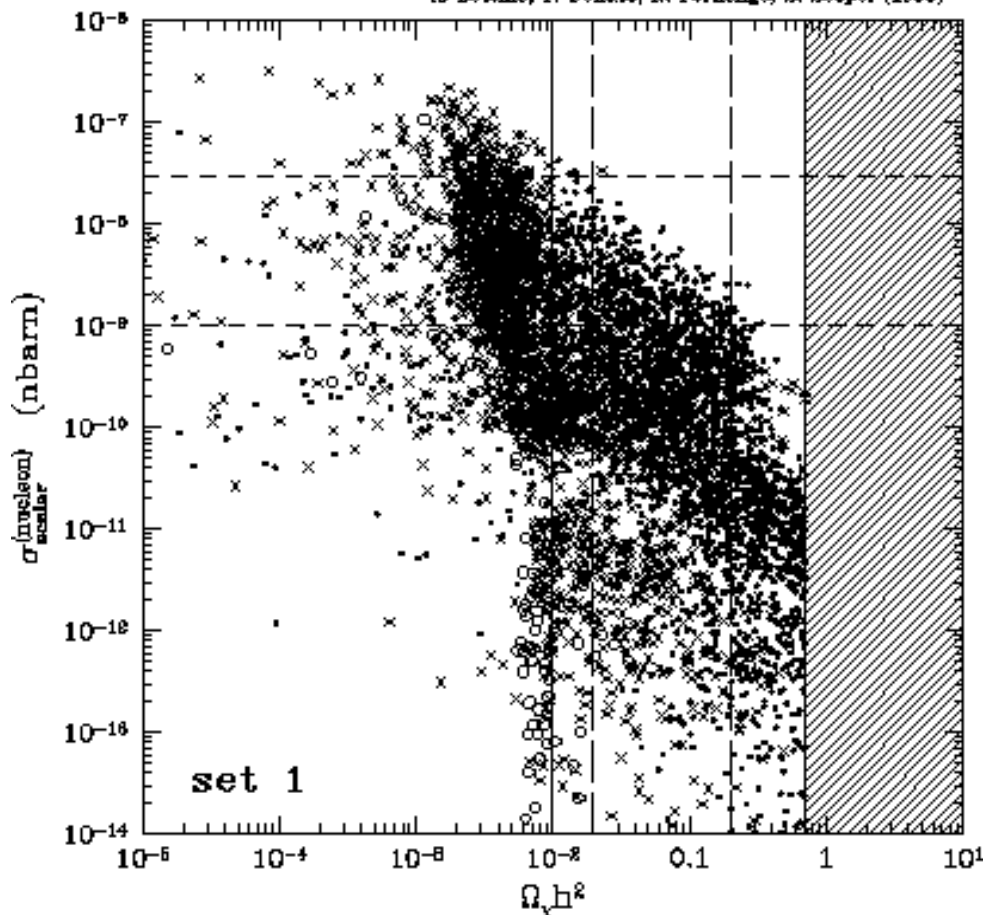


FIG.2a - Neutralino-nucleon scalar cross-section $\sigma_{\text{scalar}}^{(\text{nucleon})}$, calculated using the parameters of set 1, as a function of the neutralino relic abundance $\Omega_\chi h^2$. The two horizontal dashed lines delimit the range of the neutralino-nucleon cross section defined in Eq.(2). The two solid vertical lines delimit the interval of cosmological interest. The two vertical dashed lines delimit the preferred band for cold dark matter. The shaded region is cosmologically excluded on the basis of present limits on the age of the Universe.

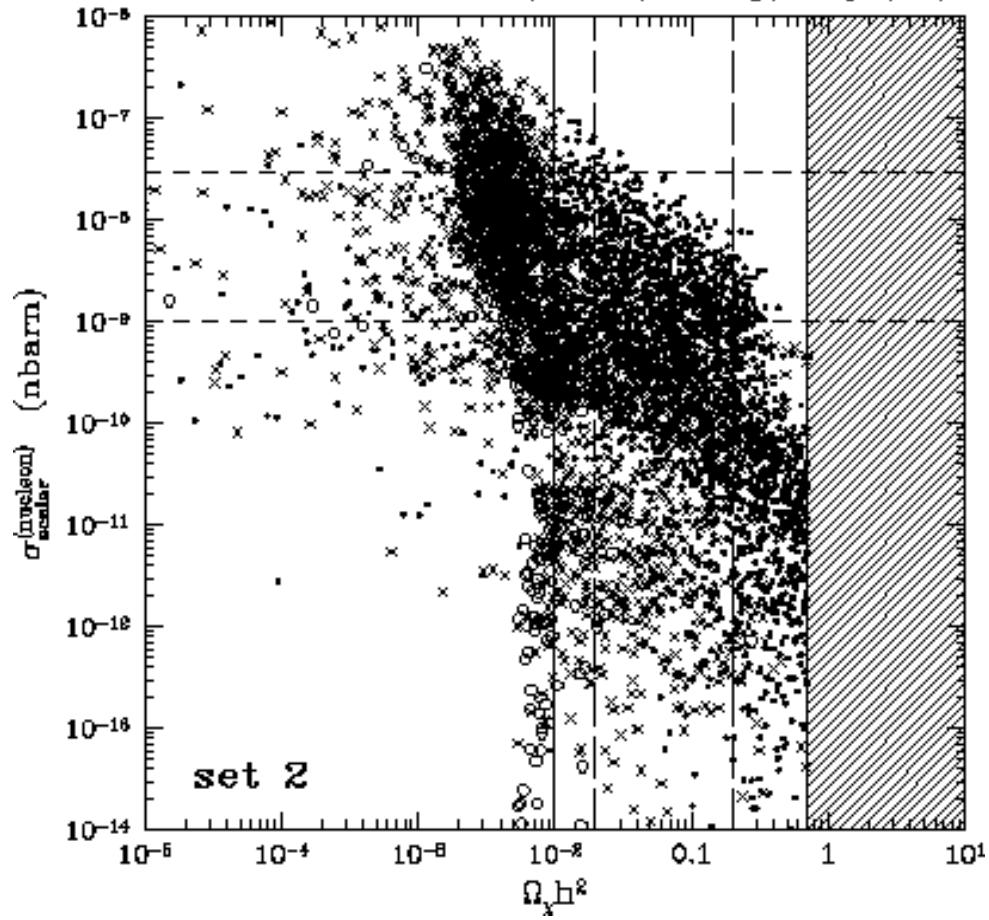


FIG.2b - The same as in Fig.2a, for the parameters of set 2.

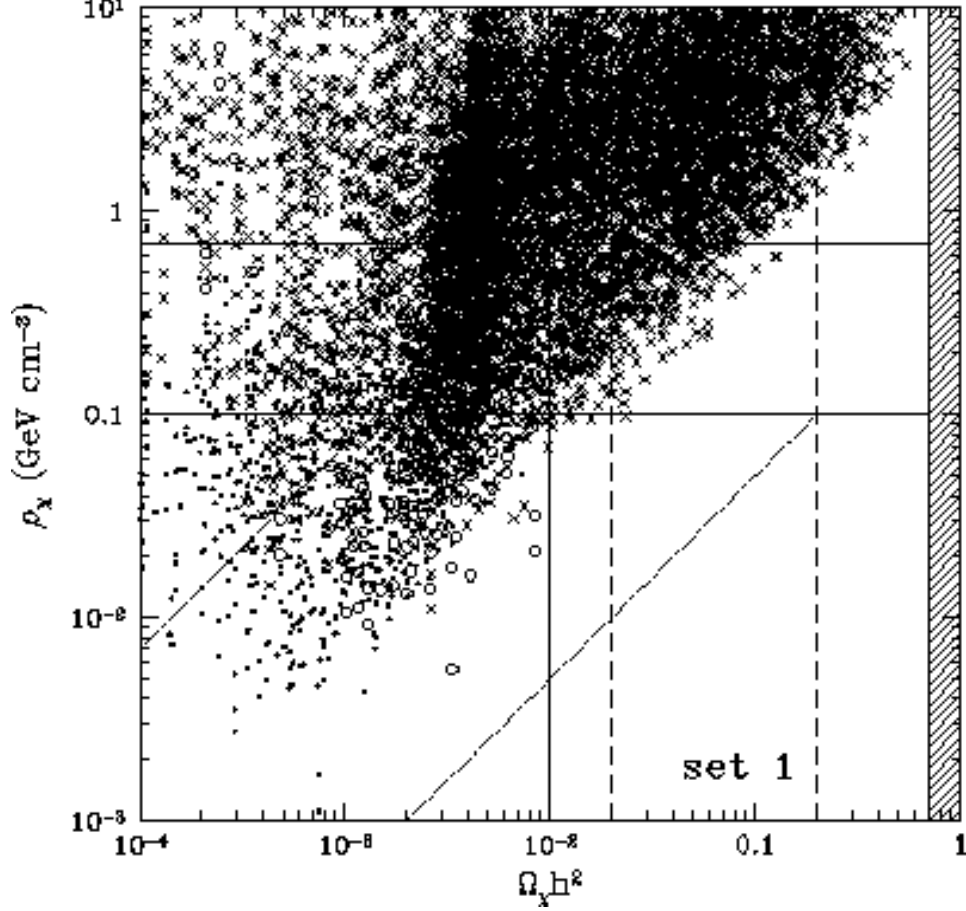


FIG.3a - Neutralino local density ρ_χ derived by requiring that $\rho_\chi \sigma_{\text{scalar}}^{(\text{nucleon})}$ falls inside the experimental DAMA region R_m , plotted against the neutralino relic abundance $\Omega_\chi h^2$. The quantity $\sigma_{\text{scalar}}^{(\text{nucleon})}$ is calculated with the parameters of set 1. The two horizontal lines delimit the physical range for the local density of non-baryonic dark matter. The two solid vertical lines delimit the interval of $\Omega_\chi h^2$ of cosmological interest. The two vertical dashed lines delimit the preferred band for cold dark matter. The two slant dot-dashed lines delimit the band where linear rescaling procedure is usually applied. The shaded region is cosmologically excluded on the basis of present limits on the age of the Universe. Different symbols identify different neutralino compositions: circles stand for a higgsino, crosses for a gaugino and dots for a mixed neutralino.

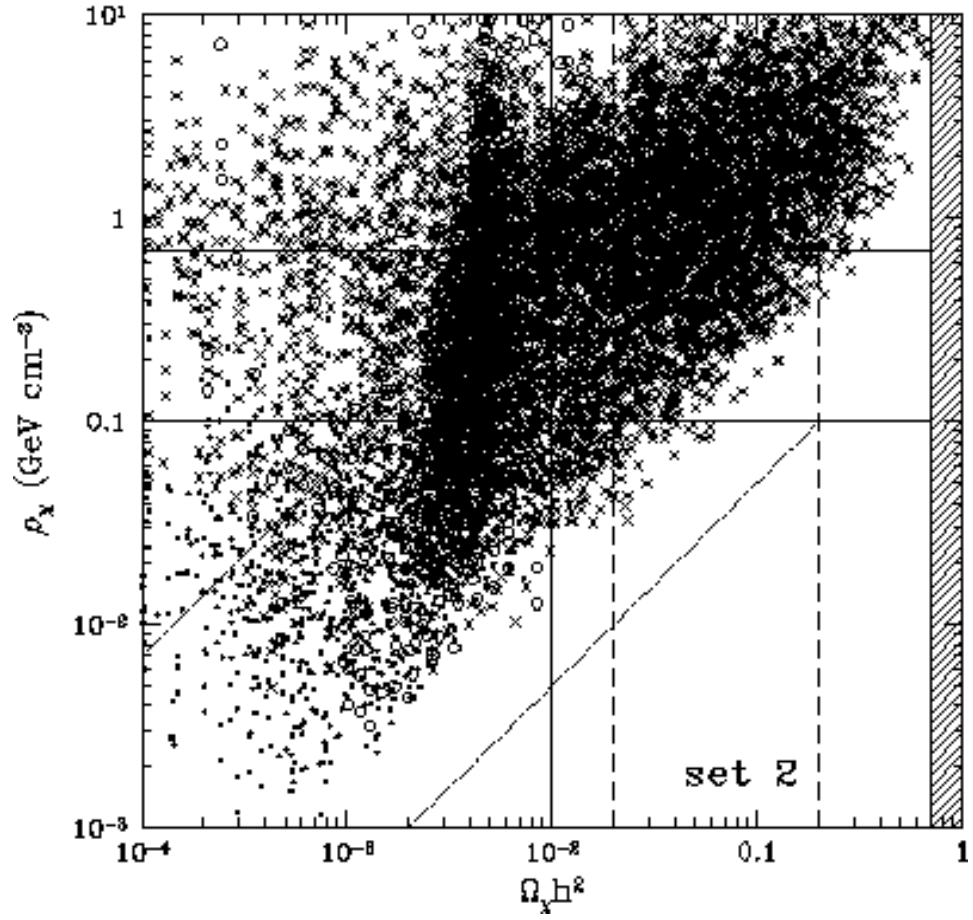


FIG.3b - The same as in Fig.3a, for the parameters of set 2.

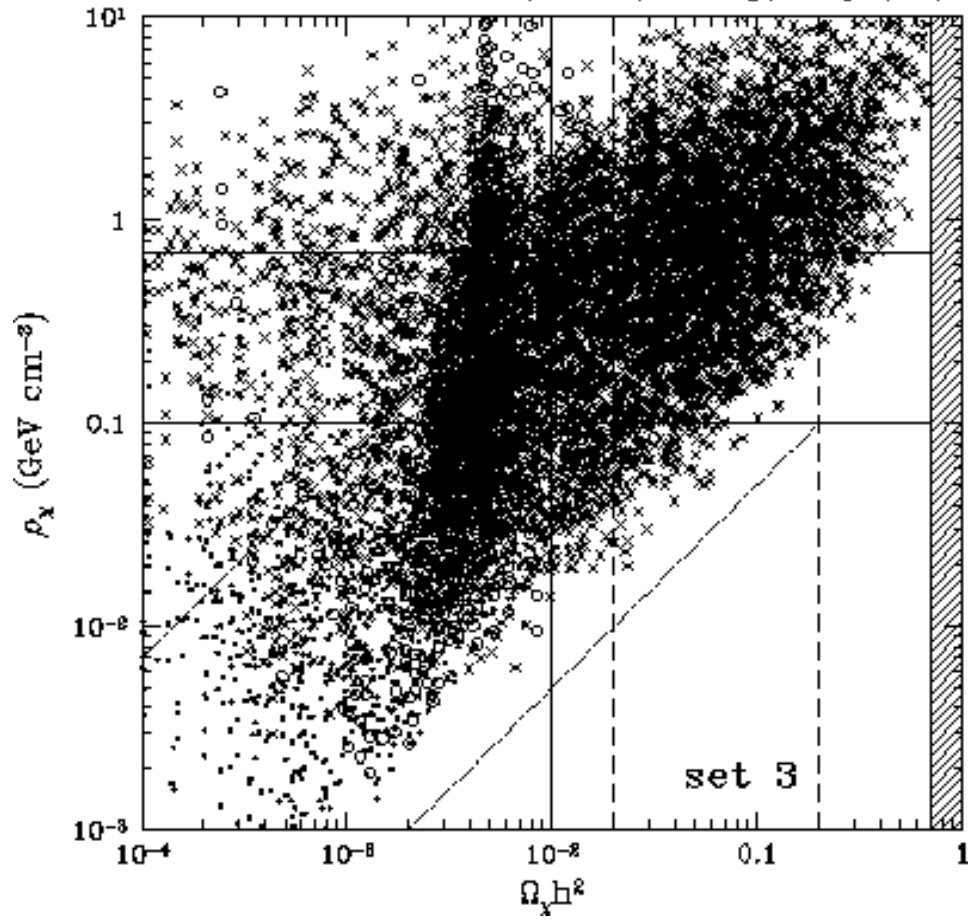


FIG.3c - The same as in Fig.3a, for the parameters of set 3.